



**Michigan
Technological
University**

Michigan Technological University
Digital Commons @ Michigan Tech

Michigan Tech Publications

11-2021

Adsorption of perfluorooctanoic acid (PFOA) and perfluorooctanesulfonic acid (PFOS) by aluminum-based drinking water treatment residuals

Zhiming Zhang
Stevens Institute of Technology

Dibyendu Sarkar
Stevens Institute of Technology

Rupali Datta
Michigan Technological Institute, rupdatta@mtu.edu

Yang Deng
Montclair State University

Follow this and additional works at: <https://digitalcommons.mtu.edu/michigantech-p>

 Part of the [Biology Commons](#)

Recommended Citation

Zhang, Z., Sarkar, D., Datta, R., & Deng, Y. (2021). Adsorption of perfluorooctanoic acid (PFOA) and perfluorooctanesulfonic acid (PFOS) by aluminum-based drinking water treatment residuals. *Journal of Hazardous Materials Letters*, 2. <http://doi.org/10.1016/j.hazl.2021.100034>
Retrieved from: <https://digitalcommons.mtu.edu/michigantech-p/16095>

Follow this and additional works at: <https://digitalcommons.mtu.edu/michigantech-p>

 Part of the [Biology Commons](#)



Adsorption of perfluorooctanoic acid (PFOA) and perfluorooctanesulfonic acid (PFOS) by aluminum-based drinking water treatment residuals

Zhiming Zhang^a, Dibyendu Sarkar^{a,*}, Rupali Datta^b, Yang Deng^{c,*}

^a Department of Civil, Environmental & Ocean Engineering, Stevens Institute of Technology, Hoboken, NJ 07030, United States

^b Department of Biological Sciences, Michigan Technological University, Houghton, MI 49931, United States

^c Department of Earth and Environmental Studies, Montclair State University, Montclair, NJ 07043, United States

ARTICLE INFO

Keywords:

PFOA
PFOS
Adsorption
Al-WTR
Water treatment

ABSTRACT

Per- and polyfluoroalkyl substances (PFAS) represent a family of emerging persistent organic pollutants. Cost-effective remediation of PFAS contamination via chemical or biochemical degradation is challenging due to their extremely high stability. This study reports the removal of two representative PFAS species, perfluorooctanoic acid (PFOA) and perfluorooctanesulfonic acid (PFOS), from water by adsorption using aluminum-based water treatment residuals (Al-WTR), a non-hazardous waste generated during the process of drinking water treatment by alum salts. Rapid adsorption of PFOA and PFOS onto Al-WTR followed a pseudo 2nd order kinetic pattern. Lower pH facilitated the adsorption process with a faster adsorption rate and greater adsorption capacity. At pH 3.0 and an initial concentration of 1.0 mg/L, 97.4 % of PFOA and 99.5 % of PFOS were adsorbed onto Al-WTR. Adsorption isotherm modeling showed that the maximum adsorption capacities of PFOA and PFOS on Al-WTR at pH 3.0 were 0.232 and 0.316 mg/g, respectively. Desorption tests indicated that the adsorption by Al-WTR was irreversible, making Al-WTR an excellent candidate for treating PFOA and PFOS in solution. The highly encouraging results of this preliminary study indicate that Al-WTR may be a promising, viable, and cost-effective PFOA/PFOS treatment option for water reuse, industrial wastewater treatment, and groundwater remediation.

1. Introduction

Per- and polyfluoroalkyl substances (PFAS) are a group of emerging persistent organic pollutants (POPs) with a perfluoroalkyl moiety in their chemical structures. Variations in functional groups and chain lengths make PFAS a complex family of chemicals, including different groups such as perfluorinated carboxylic acids (PFCAs), perfluorinated sulfonic acids (PFSAs), and perfluorinated phosphonic acids (PFPA) (Bolan et al., 2021). With their unique physical and chemical properties (e.g., persistence, hydrophobicity, and lipophobic nature), PFAS have been widely and substantially applied to industrial and commercial manufacturing since the mid-20th century (Hale et al., 2017; Buck et al., 2011). For example, the global historical PFCA production in 2005 was estimated between 4400 and 8000 tons, 3,200–7,300 tons of which eventually entered the environment via different pathways (Prevedouros et al., 2006).

As a consequence of their widespread application, PFAS have been detected in different environmental media, plants, wild animals, and

humans (Hansen et al., 2001; Bolan et al., 2021; Bulusu et al., 2020). Increasing concerns over their adverse effects on environmental and human health have led to progressively stringent PFAS-related guidelines or regulations (Hale et al., 2017; Fenton et al., 2020). For example, the U.S. Environmental Protection Agency (USEPA) has established the health advisory level of 70 ng/L for perfluorooctanoic acid (PFOA, C₇F₁₅COOH) and perfluorooctanesulfonic acid (PFOS, C₈F₁₇SO₃H) (two most prevalent PFAS species) in combination in drinking water (USEPA, 2016). However, the chemical or biochemical degradation of PFAS is exceptionally challenging due to their high stability. In contrast, adsorption provides a potentially promising remediation approach. Various adsorbent materials for immobilization of PFAS have been reported, such as alumina, boehmite, activated carbon, biochar, hematite, clays, resins, and kaolinite (Wang et al., 2021; Willemssen and Bourg, 2021; Boyer et al., 2021; Steigerwald and Ray, 2021; Wang and Shih, 2011; Wang et al., 2012; Xiao et al., 2017; Zhao et al., 2014). However, the high economic burden of using expensive adsorbents and/or their regeneration has restricted the widespread adoption of these

* Corresponding authors.

E-mail addresses: dsarkar@stevens.edu (D. Sarkar), dengy@montclair.edu (Y. Deng).

<https://doi.org/10.1016/j.hazl.2021.100034>

Received 24 May 2021; Received in revised form 28 June 2021; Accepted 13 July 2021

Available online 14 July 2021

2666-9110/© 2021 The Authors.

Published by Elsevier B.V. This is an open access article under the CC BY-NC-ND license

(<http://creativecommons.org/licenses/by-nc-nd/4.0/>).

technologies. For example, when traditional thermal regeneration of granular activated carbon (GAC) is applied, Belkouteb et al. (2020) estimated the regeneration cost of GAC filters approximately at \$0.07/m³ water with a treatment goal of 25 ng/L PFAS in a full-scale drinking water treatment plant. When the PFAS treatment goal is set at 70 ng/L (the USEPA health advisory level for combined PFOA and PFOS concentrations), McNamara et al. (2018) reported that the operation cost for GAC treatment was ~\$0.03/m³. For the regeneration of PFAS spent ion exchange resins, the overall costs are also expected to be high due to the high consumption of energy and/or chemical reagents, depending on the specific regeneration methods (Gao et al., 2021; Park et al., 2020).

Drinking water treatment residuals (WTRs) are the byproducts of the coagulation process, collected primarily after sedimentation at traditional drinking water treatment facilities. They are primarily composed of amorphous aluminum (Al) or iron (Fe) oxides/hydroxides, depending on the types of coagulants used, in addition to sediments, natural organic matter present in raw water, and occasionally, activated carbon and polymers, if dosed during water treatment (Elliott and Dempsey, 1991; Makris et al., 2006; Ippolito et al., 2011). More than 2 megatons of WTRs are generated every day in the U.S., most of which are simply landfilled (Prakash and Sengupta, 2003). Nowadays, a small fraction of WTRs is repurposed, primarily as soil amendments to immobilize phosphate in the watersheds that are highly sensitive to eutrophication (Zhou et al., 2021). Past studies, many from our group demonstrate the high adsorption capacity of WTRs for emerging organic contaminants (e. g., tetracycline and oxytetracycline) and inorganic water pollutants (e. g., As, Pb, Cu, and Zn) (Punamiya et al., 2013, 2015; Leiva et al., 2019; Soleimanifar et al., 2016; Nagar et al., 2015). The toxicity characteristic leaching protocol (TCLP) values of WTRs generated in the U.S. are well below the USEPA limits (Prakash and Sengupta, 2003; Rahmati et al., 2020). Therefore, WTR is a non-hazardous solid waste with a high potential for specific reuse in environmental remediation. Although alumina, i.e., crystalline aluminum oxide (Al₂O₃), has been reported to adsorb PFAS in water (Wang and Shih, 2011), whether the amorphous Al-oxides and hydroxides that are characteristic of WTR generated by water treatment with aluminum salts (aluminum-based WTR or Al-WTR) can similarly or better adsorb aqueous PFAS compounds remained unstudied till date.

The primary objective of this study was to evaluate the adsorption behaviors of PFOA and PFOS on a typical Al-WTR. In this study, PFOA and PFOS were selected as model PFAS species due to their prevalence and abundance in the aqueous environment (Fujii et al., 2007). Batch experiments were performed to determine adsorption kinetics and isotherm patterns. The effect of solution pH on the adsorption of PFOA and PFOS was assessed, because of its reported influence on the surface charge of Al-compounds and PFAS speciation (Wang et al., 2015).

2. Materials and methods

2.1. Materials and material pretreatment

All reagents used were analytical grade, except as noted. PFOA and PFOS were purchased from Sigma-Aldrich (St. Louis, MO, USA). HNO₃, NaOH, and NaNO₃ were obtained from Fisher Scientific (Fair Lawn, NJ, USA). Al-WTR was collected from a local drinking water treatment facility in New Jersey that uses aluminum sulfate as a primary coagulant. The air-dried ground Al-WTR was sieved through an 850- μ m sieve and then milled to micron-sized powders in a planetary ball mill following the method reported elsewhere (Balintova et al., 2012).

2.2. Adsorption experiments

Adsorption kinetic experiments were conducted in 1-L glass bottles containing 600 mL of 10 mM NaNO₃ solution (ionic strength of 10 mM) and 6.0 g of Al-WTR. Of note, PFAS concentrations in various polluted

waters are reported to vary broadly from a few ng/L to several mg/L (Crone et al., 2019; Xu et al., 2021; Anderson et al., 2016). In this study, the initial PFOA or PFOS concentration was set at 1.0 mg/L, which was reported in heavily PFAS-contaminated surface or groundwater (Anderson et al., 2016). To investigate the effect of pH on adsorption kinetics, pH levels were varied between 3.0 and 11.0 at 2-unit increments (3.0, 5.0, 7.0, 9.0, and 11.0) by adjustment with 0.1 N HNO₃ or NaOH solution. Since only a very small volume (<0.6 mL) of HNO₃ or NaOH solution was added, the effect of pH adjustment on the ionic strength was negligible (Yu et al., 2009). The bottles were shaken on a VWR Scientific orbital shaker (Philadelphia, PA, USA) at 150 rpm at 20 °C for 24 h. At different designated times (i.e., 0.0, 0.2, 0.5, 1.0, 2.0, 4.0, 7.0, 11.0, 16.0, and 24.0 h), 1.5 mL sample was collected and centrifuged immediately using an IEC Micromax microcentrifuge (International Equipment Company, MA, USA) at 16,750 g for 3 min. Filtration was avoided to prevent any potential loss of PFOA/PFOS on a filter membrane. The suspended particles were removed (described in Supplementary Information, SI) before PFOA and PFOS in the supernatant were analyzed using a Waters Quattro Ultima Mass Spectrometer (Milford, MA, USA) at selected ion monitoring mode. Control experiments were carried out under identical conditions except for no addition of Al-WTR. Results from the control showed negligible loss of the PFOA and PFOS, indicating that Al-WTR was the sole adsorbent responsible for the removal of PFOA and PFOS.

The adsorption isotherm experiment was carried out in 50 mL centrifuge tubes containing 40 mL of 10 mM NaNO₃ solution and 0.4 g of Al-WTR. Initial PFOA or PFOS concentrations were varied from 0.05, 0.1, 0.2, 0.4, 0.6, 0.8, 1.0, 1.2, to 1.5 mg/L, while the pH was adjusted between 3.0 and 11.0 at 2-unit increments for each set of experiment. Centrifuge tubes were shaken on a Glas-Col tube rotator (Terre Haute, IN, USA) at 75 rpm and 20 °C for 24 h. Preliminary studies showed that a pseudo-equilibrium status was attained within 24-h shaking (i.e., no further adsorption). Following shaking, the tubes were centrifuged using an Eppendorf centrifuge 5804 at 3000 g for 30 min (Eppendorf, CT, USA) before the supernatant was collected for PFOA or PFOS analysis (described in SI) (Wang et al., 2021). Both adsorption kinetic and isotherm studies were performed in triplicates. All data shown in the figures represent the arithmetic means of triplicate measurements with error bars indicating standard deviations.

2.3. Desorption experiment

After the adsorption experiments, the PFOA or PFOS loaded Al-WTR was separated by completely decanting the liquid. Thereafter, 40 mL of 0.1 mM NaNO₃ solution was added to each centrifuge tube before the pH was adjusted. After another 24-h shaking at 75 rpm at 20 °C on the end-over-end shaker, the tubes were centrifuged again at 3000 g for 30 min (Eppendorf, CT, USA), before the supernatant was collected for analysis. Because masses of the tube and Al-WTR remained constant, PFOA or PFOS bound to Al-WTR after the desorption experiments could be calculated by mass balance via determination of the mass difference between the initial adsorbed amount on Al-WTR and the desorbed amount in the supernatant (Wang et al., 2021). The desorption tests were also performed in triplicates.

2.4. Material characterization

To gain the morphological, elemental, and crystal structure information, Al-WTR was characterized using a Scanning Electron Microscope (SEM, FEI Nova 400 Nano SEM, FEI, USA) with Energy Dispersive X-ray (EDX) and a Powder X-Ray Diffractometer (XRD, Rigaku SmartLab XRD, USA), respectively. ICDD database was used for XRD data analysis in Rigaku Smartlab Studio II. Point of zero charge (pH_{pzc}) and particle size of Al-WTR were measured by Zetasizer Nano ZS (ZEN 3600, Malvern, USA) (Wang et al., 2015). Fourier-transform infrared spectroscopy (FTIR, Thermo Scientific Nicolet iS50, USA) was used to identify the

change of surface functional groups over the adsorption.

3. Results and discussion

3.1. Al-WTR characterization

FTIR spectra (Fig. S1) identified three major peaks in Al-WTR, corresponding to the presence of inorganic silica (1000 cm^{-1}), -OH (1410 cm^{-1}), and COO^- (1560 cm^{-1}) groups (Barden et al., 2015; Painter et al., 2012; Grigorenko et al., 2017). Though Al-WTR was mostly amorphous, XRD showed some crystallized quartz and calcium aluminum silicate peaks (Fig. S2), consistent with the SEM imaging and EDX mapping spectra indicating that the major elements were Si, O, and Al (Fig. S3). Because of the absence of crystalline Al-O, Al in the Al-WTR can be assumed to predominantly exist as amorphous Al oxides/hydroxides, which is consistent with previous reports (Ippolito et al., 2011; Dayton and Basta, 2005). The diameter of Al-WTR particles had a Z-average of $1.2\ \mu\text{m}$ and polydispersity index (PDI) of 0.12. The pH_{pzc} of Al-WTR was determined to be 7.1.

3.2. Adsorption kinetics

Kinetics of adsorption of PFOA and PFOS by Al-WTR are shown in Fig. 1. Adsorption equilibrium for both PFOA and PFOS was reached within 2 h. It was similar to that of powdered activated carbon (PAC) (size $<100\ \mu\text{m}$), but less than those of GAC (average size $900\text{--}1000\ \mu\text{m}$), alumina (average size $87\ \mu\text{m}$), and boehmite (average size $37\ \mu\text{m}$), at similar adsorption experimental conditions (Yu et al., 2009; Wang and Shih, 2011; Wang et al., 2012). Both the material properties and size may contribute to the difference in adsorption performance. Approximately 92 % of PFOA and 98 % of PFOS were adsorbed in the first 0.2 h, particularly at the lowest pH of 3.0, indicating a fast adsorption process, which suggested that the adsorption of PFOA and PFOS significantly depended on the available binding sites on Al-WTR (Ayub et al., 2020). A new peak in the FTIR spectra was observed at 1340 cm^{-1} after PFOA or PFOS adsorption on Al-WTR (Fig. S1), corresponding to the -CF_2 band (Gao and Chorover, 2012), validating the occurrence of PFOA or PFOS adsorption on Al-WTR. PFOS adsorption ($99.5 \pm 0.1\%$) was slightly greater than PFOA adsorption ($97.4 \pm 0.3\%$) at pH 3.0, which can possibly be ascribed to the different head groups of PFOA and PFOS sharing the same fluoroalkyl tail (Wang and Shih, 2011). The greater degree of affinity between aluminum oxide of Al-WTR and the sulfonic group of PFOS that is more electronegative than the carboxylic group of PFOA (Xing et al., 2020; Schmitt and Pietrzyk, 1985) may contribute to greater adsorption of PFOS by Al-WTR. Another plausible reason is the stronger hydrophobicity of PFOS (Xing et al., 2020). In this study, the PFOA and PFOS removal due to the formation of micelles or hemi-micelles was insignificant. The initial concentrations (1.0 mg/L) were much lower than their respective critical micelle concentrations (PFOA: $15,696$; and PFOS: $4,573\text{ mg/L}$) (Yu et al., 2009; Johnson et al.,

2007). Moreover, PFOA or PFOS hemi-micelles were not expected to form at such a low concentration (Johnson et al., 2007).

To further explore the adsorption kinetics, experimental data were fitted to the pseudo 1st and 2nd order kinetic models as described in SI. As illustrated by Fig. S4 with the key model parameters summarized in Table 1, at pH 3.0, both PFOA or PFOS adsorption followed the pseudo 2nd order kinetic model ($R^2 = 1.000$) better than the pseudo 1st order kinetic model ($R^2 < 0.280$). The experimentally measured q_e was consistent with q_e determined from the 2nd-order kinetic model with very small relative errors ($<2\%$ for PFOA and $<1\%$ for PFOS). The simulated adsorption capacities, 0.097 mg/g for PFOA and 0.099 mg/g for PFOS, were close to the experimental data, 0.097 mg/g for PFOA and 0.100 mg/g for PFOS. The pseudo 2nd order kinetic model also better represented adsorption at other pH levels in terms of R^2 and the consistency between measured and simulated q_e (Table 1). A better degree of fit of the pseudo 2nd order kinetic model was consistent with data reported in the literature that used other adsorbents (e.g., GAC and biochar) for PFOA and PFOS adsorption (Zhang et al., 2019a,b). This also indicated that the adsorption of both PFOA and PFOS on Al-WTR was controlled by chemical adsorption, and the number of binding sites on Al-WTR played a vital role on the degree of adsorption. The greater adsorption capacity of PFOS compared to PFOA and faster adsorption kinetics were in line with previously reported adsorption studies using other adsorbents (Zhang et al., 2019a,b; Xu et al., 2015; Wang and Shih, 2011).

3.3. Adsorption isotherms

Adsorption isotherms of PFOA and PFOS on Al-WTR (described in SI) at pH 3.0 are shown in Fig. S5. Data in both Table 1 and Fig. S5 indicate that the Langmuir isotherm models were slightly better fitted to PFOA and PFOS adsorption than the Freundlich isotherm models, though both models yielded R^2 values that were high and significant (at $p < 0.05$) regardless of pH. This finding suggests that the adsorption of PFOA or PFOS molecules may be occurring on the surface of Al-WTR with a monolayer coverage (Ünlü and Ersoz, 2006; Rattanaoudom et al., 2012; Xu et al., 2015; Wang et al., 2012).

The dimensionless Langmuir constants, R_L , varied between $0.106\text{--}0.171$ and $0.041\text{--}0.108$ for PFOA and PFOS, respectively, at the various pH levels, indicating that adsorption was favorable for both chemicals (Ayub et al., 2020; Meroufel et al., 2013). The maximum adsorption capacities of PFOA and PFOS on Al-WTR were estimated to be 0.232 and 0.316 mg/g , respectively, at pH 3.0 by the Langmuir model (Table 1). The maximum adsorption capacities of Al-WTR were greater than that of alumina reported elsewhere (0.014 and 0.022 mg/g for PFOA and PFOS, respectively, at pH 4.3, Wang and Shih, 2011). At pH 7.0, Al-WTR (Table 1) exhibited similar maximum adsorption capacities for PFOA and PFOS with boehmite (0.189 and 0.262 mg/g for PFOA and PFOS, respectively, Wang et al., 2012). In contrast, though Al-WTR and PAC shared the similar duration to reach adsorption equilibria, PAC was

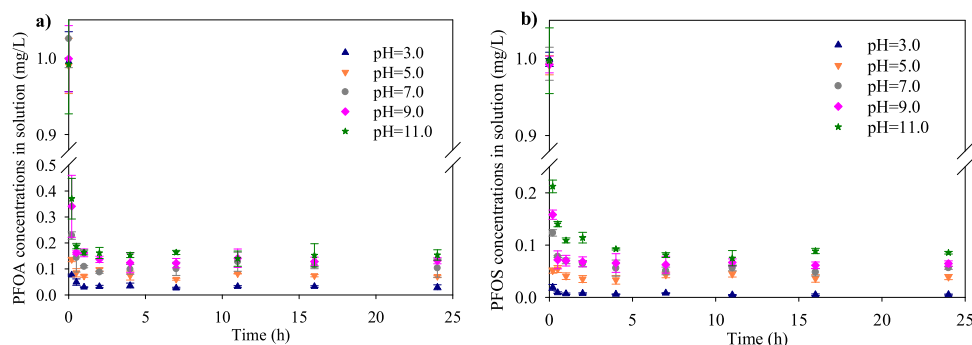


Fig. 1. Kinetics of PFOA and PFOS adsorption on Al-WTR.

Table 1
Kinetic and isotherm parameters for PFOA and PFOS adsorption on Al-WTR.

Isotherm and kinetic models	Parameters	pH = 3.0		pH = 5.0		pH = 7.0		pH = 9.0		pH = 11.0	
		PFOA	PFOS								
q _e , experiment (mg/g)		0.097 (0.000)	0.100 (0.000)	0.093 (0.000)	0.096 (0.001)	0.094 (0.001)	0.094 (0.000)	0.087 (0.000)	0.094 (0.001)	0.085 (0.002)	0.091 (0.001)
	q _e , simulation (mg/g)	0.003 (0.001)	0.001 (0.000)	0.005 (0.001)	0.002 (0.001)	0.007 (0.002)	0.003 (0.000)	0.008 (0.003)	0.003 (0.001)	0.006 (0.003)	0.005 (0.002)
Pseudo 1 st order	k ₁ (min ⁻¹)	0.086 (0.013)	0.132 (0.029)	0.092 (0.019)	0.067 (0.011)	0.078 (0.008)	0.119 (0.024)	0.194 (0.023)	0.104 (0.016)	0.113 (0.016)	0.136 (0.025)
	R ² (p < 0.05)	0.205 (0.053)	0.278 (0.051)	0.264 (0.061)	0.119 (0.027)	0.216 (0.116)	0.216 (0.075)	0.593 (0.110)	0.266 (0.052)	0.331 (0.065)	0.328 (0.096)
	q _e , simulation (mg/g)	0.097 (0.001)	0.099 (0.000)	0.092 (0.000)	0.095 (0.001)	0.092 (0.002)	0.094 (0.000)	0.087 (0.001)	0.093 (0.000)	0.084 (0.002)	0.091 (0.000)
Pseudo 2 nd order	k ₂ (g/mg-min)	1402 (164)	2842 (273)	837 (126)	2307 (139)	797 (121)	1916 (188)	700 (58)	1525 (109)	641 (47)	1237 (117)
	R ² (p < 0.05)	1.000 (0.000)	1.000 (0.000)	1.000 (0.000)	1.000 (0.000)	1.000 (0.001)	1.000 (0.000)	1.000 (0.000)	1.000 (0.000)	1.000 (0.001)	1.000 (0.000)
	q _{max} (mg/g)	0.232 (0.011)	0.316 (0.027)	0.192 (0.022)	0.253 (0.018)	0.180 (0.011)	0.235 (0.014)	0.149 (0.015)	0.204 (0.008)	0.139 (0.013)	0.184 (0.018)
Langmuir	K _L (L/mg)	6.771 (1.380)	29.486 (1.591)	8.416 (0.233)	11.359 (0.707)	6.263 (0.348)	11.375 (1.029)	5.405 (0.385)	13.053 (1.742)	4.844 (1.047)	10.371 (1.090)
	R _L	0.129 (0.069)	0.041 (0.011)	0.106 (0.029)	0.099 (0.016)	0.138 (0.026)	0.099 (0.047)	0.156 (0.063)	0.087 (0.041)	0.171 (0.021)	0.108 (0.028)
	R ² (p < 0.05)	0.995 (0.006)	0.953 (0.020)	0.991 (0.027)	0.982 (0.015)	0.970 (0.040)	0.990 (0.009)	0.968 (0.048)	0.993 (0.004)	0.943 (0.041)	0.985 (0.008)
	K _f	1.243 (0.171)	10.693 (1.378)	0.629 (0.052)	3.535 (0.186)	0.626 (0.062)	2.291 (0.400)	0.544 (0.078)	1.772 (0.313)	0.452 (0.133)	1.613 (0.351)
	1/n	0.977 (0.033)	1.026 (0.026)	0.829 (0.018)	1.062 (0.015)	0.893 (0.059)	0.994 (0.044)	0.938 (0.066)	0.948 (0.048)	0.931 (0.073)	0.997 (0.068)
Freundlich		0.977 (0.033)	1.026 (0.026)	0.829 (0.018)	1.062 (0.015)	0.893 (0.059)	0.994 (0.044)	0.938 (0.066)	0.948 (0.048)	0.931 (0.073)	0.997 (0.068)
	R ² (p < 0.05)	0.994 (0.002)	0.921 (0.022)	0.990 (0.004)	0.986 (0.008)	0.977 (0.046)	0.995 (0.006)	0.971 (0.028)	0.995 (0.003)	0.961 (0.010)	0.957 (0.016)

Note: Standard deviations are shown in the parentheses.

reported to have much higher maximum adsorption capacities for both PFOA (~277 mg/g) and PFOS (~520 mg/g) (Yu et al., 2009).

3.4. Effect of solution pH

The effects of pH on PFOA and PFOS adsorption kinetics and capacities are shown in Figs. 1 and 2, respectively. Regardless of the chemical, lower pH led to more rapid adsorption and greater adsorption capacity. Specifically, with the increase in solution pH, adsorption for PFOA decreased from ~97.4 % at pH 3.0 to ~84.6 % at pH 11.0 and from ~99.5 % to ~91.5 % for PFOS. The pseudo 2nd order kinetic rate constants decreased from 1402 to 641 g/min and from 2842 to 1237 g/mg-min for PFOA and PFOS, respectively, with pH increase from 3.0 to 11.0 (Table 1). At a given pH level, the rate constant for PFOS was higher than that of PFOA, indicating faster adsorption. Adsorption capacities at experimental conditions for both PFOA and PFOS decreased with an increase in pH (Fig. 2); the trend was the same for maximum adsorption capacity q_{max}. The q_{max} of PFOA and PFOS declined from 0.232 to 0.139 mg/g and from 0.316 to 0.184 mg/g, respectively, with a pH increase

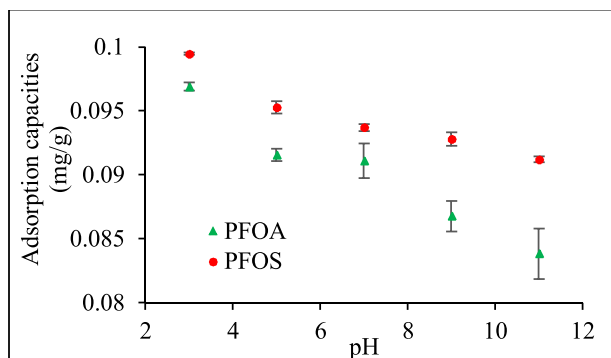


Fig. 2. Effect of pH on the adsorption of PFOA and PFOS on Al-WTR.

from 3.0 to 11.0 (Table 1).

Solution pH can influence the speciation of PFOA and PFOS as well as the surface charge on Al-WTR. At the experimental conditions (pH 3.0–11.0), PFOA and PFOS principally exist in their respective deprotonated forms (pK_a = 2.5 for PFOA and -3.3 for PFOS) (Yu et al., 2009). Meanwhile, pH_{pzc} of Al-WTR was 7.1. Therefore, the adsorption of deprotonated PFOA or PFOS was not favored at higher pH, because the surface charge of Al-WTR became less positive with the pH increase at pH < pH_{pzc} and more negative with the pH increase at pH > pH_{pzc} (Wang and Shih, 2011). The small diameter of the amorphous Al oxides/hydroxides particles at Z-average of 1.2 μm implies a large specific surface area. Hence, although electrostatic attraction diminished at higher pH conditions, the amorphous Al oxides/hydroxides particles could still facilitate the adsorption of PFOA and PFOS via other mechanisms that are discussed in the following section.

3.5. Desorption of PFOA and PFOS from Al-WTR

Desorption of PFOA and PFOS from Al-WTR for samples at pH 3.0 and initial concentrations of 0.05–1.5 mg/L is shown in Fig. 3a. Desorbed PFOS fraction accounted for <1.1 % of the total adsorbed PFOS at various initial concentrations, indicating that the adsorption is hysteretic. The fraction of desorbed PFOA ranged from 5.6 % to 11.8 % with variation in the initial PFOA concentration, also suggesting hysteretic adsorption. The stronger affinity of Al-WTR toward PFOS than PFOA can possibly be ascribed to the lower solubility and higher hydrophobicity of PFOS. Similar findings were reported elsewhere for other adsorbents (Milinovic et al., 2015; Askeland et al., 2020). Although the adsorption rates and capacities decreased along with an increase in pH (Figs. 1 and 2, Table 1), adsorption was irreversible once PFOA and PFOS were adsorbed by Al-WTR at all pH levels. This again implies that the binding was principally governed by chemisorption and not electrostatic attraction.

As Fig. 3b demonstrates, less than 8.1 % of the adsorbed PFOA and less than 1.9 % of the adsorbed PFOS desorbed at all five pH levels.

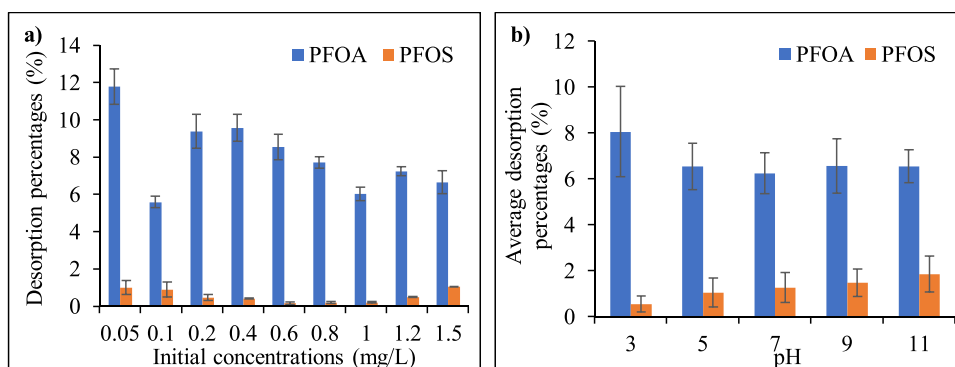


Fig. 3. a) Percentages of PFOA and PFOS desorbed from Al-WTR at pH 3.0, and b) average desorption percentages for all PFOA and PFOS concentrations at each pH level.

Generally, there was no significant difference in PFOA or PFOS desorption at different pH conditions. Although a certain degree of electrostatic repulsion was reported for PFOA or PFOS on negatively charged adsorbents (Yu et al., 2009; Chen et al., 2011), PFOA or PFOS was still adsorbed by those adsorbents (e.g., carbon nanotubes, chars, activated sludge, and metal oxides) (Zhang et al., 2019a,b; Chen et al., 2011; Zhou et al., 2010), suggesting that in addition to just electrostatic interactions chemisorption mechanisms were also involved and governed the surface complexation of the adsorbents with aqueous PFOA or PFOS (Zhang et al., 2019a,b). This may explain the apparent lack of pH dependence of PFOA or PFOS desorption from Al-WTR.

Of interest, the pH dependence pattern was observed at the adsorption phase, but not during the ensuing desorption stage. The plausible reason is the transition of dominant adsorption pathways. In the initial adsorption step, electrostatic columbic interactions are a prerequisite condition enabling the association of PFOA/PFOS in bulk solution and WTR surface. The physical adsorption occurring on the adsorbent surface is highly pH-dependent and reversible. Thereafter, strong chemical bonds form to attain irreversible chemical adsorption, which is typically slower than the initial physical adsorption. A similar adsorption procedure was reported in arsenic sorption to nano zero-valent iron modified activated carbon (Zhu et al., 2009).

Although elucidation of the underlying adsorption mechanisms was out of the scope of this preliminary study, Al-WTR can possibly immobilize PFOA and PFOS through the formation of inner or outer-sphere complexes between PFAS molecules and surface functional groups on Al-WTR (Gao and Chorover, 2012) and/or hydrophobic interactions (Lin et al., 2015). Particularly, the inner-sphere complex by ion exchange can lead to strong adsorption with little desorption. In contrast, PFOA and PFOS have a hydrophilic functional head and a hydrophobic fluoroalkyl tail (Buck et al., 2011), the latter facilitating their association with a solid phase. Besides the amorphous aluminum hydroxides, hydrophobic natural organic matter, which phase-transferred from raw water to WTR during the alum coagulation process, can also contribute to PFOA and PFOS adsorption via hydrophobic interactions. A more detailed mechanistic investigation is in progress to further elucidate the interactions between Al-WTR and PFOA and PFOS species.

4. Conclusion

This paper reports for the first time, the rapid and effective adsorption of PFOA and PFOS by Al-WTR, a non-hazardous industrial solid waste. The PFOA/PFOS adsorption rate and capacity were higher at lower pH. Once adsorbed, little PFOA or PFOS desorption occurred, regardless of pH, indicating hysteretic adsorption, plausibly due to the formation of inner- and outer-sphere surface complexes and/or hydrophobic interactions. The low cost of Al-WTR (a solid waste) makes the treatment process economically competitive, thereby making it a treatment of choice over most other currently available PFAS treatment

technologies. Additionally, the beneficial reuse of an industrial waste for addressing water pollution by persistent emerging contaminants provides a sustainable approach to non-hazardous solid waste management. Therefore, Al-WTR-based adsorption may be developed into a promising, viable, and cost-effective technology that is capable of alleviating PFAS contamination problems in various scenarios, such as water reuse, industrial wastewater treatment, and groundwater remediation.

Funding

This research did not receive any specific grant from funding agencies in the public, commercial, or not-for-profit sectors.

Author contributions

Zhiming Zhang: Methodology, Data Curation, Writing - Original Draft Preparation, Visualization. **Dibyendu Sarkar:** Conceptualization, Methodology, Supervision, Writing - Review & Editing, Visualization. **Rupali Datta:** Writing - Review & Editing, Visualization. **Yang Deng:** Writing - Review & Editing, Visualization.

Declaration of Competing Interest

The authors declare no conflict of interest.

Acknowledgments

The authors thank Dr. Athula Attygalle and Zhaoyu Zheng at Stevens Institute of Technology for help in PFOA and PFOS analysis. The authors also thank Sameer Neve and Mohammad Halim at Stevens Institute of Technology for their technical help.

Appendix A. Supplementary data

Supplementary material related to this article can be found, in the online version, at doi:<https://doi.org/10.1016/j.hazl.2021.100034>.

References

- Anderson, R.H., Long, G.C., Porter, R.C., Anderson, J.K., 2016. Occurrence of select perfluoroalkyl substances at U.S. Air Force aqueous film-forming foam release sites other than fire-training areas: field-validation of critical fate and transport properties. *Chemosphere* 150, 678–685.
- Askeland, M., Clarke, B.O., Cheema, S.A., Mendez, A., Gasco, G., Paz-Ferreiro, J., 2020. Biochar sorption of PFOS, PFOA, PFHxS and PFHxA in two soils with contrasting texture. *Chemosphere* 249, 126072.
- Ayub, A., Raza, Z.A., Majeed, M.I., Tariq, M.R., Irfan, A., 2020. Development of sustainable magnetic chitosan biosorbent beads for kinetic remediation of arsenic contaminated water. *Int. J. Biol. Macromol.* 163, 603–617.
- Balintova, M., Holub, M., Singovszka, E., 2012. Study of iron, copper and zinc removal from acidic solutions by sorption. *Chem. Eng. Trans.* 28, 175–180.

- Barden, H.E., Behnsen, J., Bergmann, U., Leng, M.J., Manning, P.L., Withers, P.J., et al., 2015. Geochemical evidence of the seasonality, affinity and pigmentation of *Solenopora jurassica*. *PLoS One* 10 (9), e0138305.
- Belkouteb, N., Franke, V., McCleaf, P., Köhler, S., Ahrens, L., 2020. Removal of per-and polyfluoroalkyl substances (PFASs) in a full-scale drinking water treatment plant: long-term performance of granular activated carbon (GAC) and influence of flow-rate. *Water Res.* 182, 115913.
- Bolan, N., Sarkar, B., Yan, Y., Li, Q., Wijesekera, H., Kannan, K., et al., 2021. Remediation of poly-and perfluoroalkyl substances (PFAS) contaminated soils—To mobilize or to immobilize or to degrade? *J. Hazard. Mater.* 401, 123892.
- Boyer, T.H., Fang, Y., Ellis, A., Dietz, R., Choi, Y.J., Schaefer, C.E., et al., 2021. Anion exchange resin removal of per-and polyfluoroalkyl substances (PFAS) from impacted water: a critical review. *Water Res.*, 117244.
- Buck, R.C., Franklin, J., Berger, U., Conder, J.M., Cousins, I.T., De Voogt, P., et al., 2011. Perfluoroalkyl and polyfluoroalkyl substances in the environment: terminology, classification, and origins. *Integr. Environ. Assess. Manag.* 7 (4), 513–541.
- Bulusu, R.K., Wandell, R.J., Zhang, Z., Farahani, M., Tang, Y., Locke, B.R., 2020. Degradation of PFOA with a nanosecond-pulsed plasma gas-liquid flowing film reactor. *Plasma Processes Polym.* 17 (8), e2000074.
- Chen, X., Xia, X., Wang, X., Qiao, J., Chen, H., 2011. A comparative study on sorption of perfluorooctane sulfonate (PFOS) by chars, ash and carbon nanotubes. *Chemosphere* 83 (10), 1313–1319.
- Crone, B.C., Speth, T.F., Wahman, D.G., Smith, S.J., Abulikemu, G., Kleiner, E.J., Pressman, J.G., 2019. Occurrence of per-and polyfluoroalkyl substances (PFAS) in source water and their treatment in drinking water. *Crit. Rev. Environ. Sci. Technol.* 49 (24), 2359–2396.
- Dayton, E.A., Basta, N.T., 2005. A method for determining the phosphorus sorption capacity and amorphous aluminum of aluminum-based drinking water treatment residuals. *J. Environ. Qual.* 34 (3), 1112–1118.
- Elliott, H.A., Dempsey, B.A., 1991. Agronomic effects of land application of water treatment sludges. *J.-Am. Water Works Assoc.* 83 (4), 126–131.
- Fenton, S.E., Ducatman, A., Boobis, A., DeWitt, J.C., Lau, C., Ng, C., et al., 2020. Per-and polyfluoroalkyl substance toxicity and human health review: current state of knowledge and strategies for informing future research. *Environ. Toxicol. Chem.*
- Fujii, S., Polprasert, C., Tanaka, S., Hong Lien, N.P., Qiu, Y., 2007. New POPs in the water environment: distribution, bioaccumulation and treatment of perfluorinated compounds—a review paper. *J. Water Supply Res. Technol. AQUA* 56 (5), 313–326.
- Gao, X., Chorover, J., 2012. Adsorption of perfluorooctanoic acid and perfluorooctanesulfonic acid to iron oxide surfaces as studied by flow-through ATR-FTIR spectroscopy. *Environ. Chem.* 9 (2), 148–157.
- Gao, P., Cui, J., Deng, Y., 2021. Direct regeneration of ion exchange resins with sulfate radical-based advanced oxidation for enabling a cyclic adsorption–regeneration treatment approach to aqueous perfluorooctanoic acid (PFOA). *Chem. Eng. J.* 405, 126698.
- Grigorenko, V.G., Andreeva, I.P., Rubtsova, M.Y., Deygen, I.M., Antipin, R.L., Majouga, A.G., et al., 2017. Novel non-β-lactam inhibitor of β-lactamase TEM-171 based on acylated phenoxyaniline. *Biochimie* 132, 45–53.
- Hale, S.E., Arp, H.P.H., Slind, G.A., Wade, E.J., Bjørseth, K., Breedveld, G.D., et al., 2017. Sorbent amendment as a remediation strategy to reduce PFAS mobility and leaching in a contaminated sandy soil from a Norwegian firefighting training facility. *Chemosphere* 171, 9–18.
- Hansen, K.J., Clemen, L.A., Ellefson, M.E., Johnson, H.O., 2001. Compound-specific, quantitative characterization of organic fluorochemicals in biological matrices. *Environ. Sci. Technol.* 35 (4), 766–770.
- Ippolito, J.A., Barbarick, K.A., Elliott, H.A., 2011. Drinking water treatment residuals: a review of recent uses. *J. Environ. Qual.* 40 (1), 1–12.
- Johnson, R.L., Anschutz, A.J., Smolen, J.M., Simcik, M.F., Penn, R.L., 2007. The adsorption of perfluorooctane sulfonate onto sand, clay, and iron oxide surfaces. *J. Chem. Eng. Data* 52 (4), 1165–1170.
- Leiva, J.A., Wilson, P.C., Albano, J.P., Nkedi-Kizza, P., O'Connor, G.A., 2019. Pesticide sorption to soilless media components used for ornamental plant production and aluminum water treatment residuals. *ACS Omega* 4 (18), 17782–17790.
- Lin, H., Wang, Y., Niu, J., Yue, Z., Huang, Q., 2015. Efficient sorption and removal of perfluoroalkyl acids (PFAAs) from aqueous solution by metal hydroxides generated in situ by electrocoagulation. *Environ. Sci. Technol.* 49 (17), 10562–10569.
- Makris, K.C., Sarkar, D., Datta, R., 2006. Evaluating a drinking-water waste by-product as a novel sorbent for arsenic. *Chemosphere* 64 (5), 730–741.
- McNamara, J.D., Franco, R., Mimna, R., Zappa, L., 2018. Comparison of activated carbons for removal of perfluorinated compounds from drinking water. *J.-Am. Water Works Assoc.* 110 (1), E2–E14.
- Meroufel, B., Benali, O., Benyahia, M., Benmoussa, Y., Zenasni, M.A., 2013. Adsorptive removal of anionic dye from aqueous solutions by Algerian kaolin: characteristics, isotherm, kinetic and thermodynamic studies. *J. Mater. Environ. Sci.* 4 (3), 482–491.
- Milinic, J., Lacorte, S., Vidal, M., Rigol, A., 2015. Sorption behaviour of perfluoroalkyl substances in soils. *Sci. Total Environ.* 511, 63–71.
- Nagar, R., Sarkar, D., Punamiya, P., Datta, R., 2015. Drinking water treatment residual amendment lowers inorganic arsenic bioaccessibility in contaminated soils: a long-term study. *Water Air Soil Pollut.* 226 (11), 366.
- Painter, P.C., Starsinic, M., Coleman, M.M., 2012. Determination of functional groups in coal by Fourier transform interferometry. *Fourier Transform Infrared Spectrosc.* 4, 169–240.
- Park, M., Daniels, K.D., Wu, S., Ziska, A.D., Snyder, S.A., 2020. Magnetic ion-exchange (MIEX) resin for perfluorinated alkylsubstance (PFAS) removal in groundwater: roles of atomic charges for adsorption. *Water Res.* 181, 115897.
- Prakash, P., SenGupta, A.K., 2003. Selective coagulant recovery from water treatment plant residuals using Donnan membrane process. *Environ. Sci. Technol.* 37 (19), 4468–4474.
- Prevedourous, K., Cousins, I.T., Buck, R.C., Korzeniowski, S.H., 2006. Sources, fate and transport of perfluorocarboxylates. *Environ. Sci. Technol.* 40 (1), 32–44.
- Punamiya, P., Sarkar, D., Rakshit, S., Datta, R., 2013. Effectiveness of aluminum-based drinking water treatment residuals as a novel sorbent to remove tetracyclines from aqueous medium. *J. Environ. Qual.* 42 (5), 1449–1459.
- Punamiya, P., Sarkar, D., Rakshit, S., Datta, R., 2015. Effect of solution properties, competing ligands, and complexing metal on sorption of tetracyclines on Al-based drinking water treatment residuals. *Environ. Sci. Pollut. Res.* 22 (10), 7508–7518.
- Rahmati, R., Sarkar, D., Na Nagara, V., Zhang, Z., Datta, R., 2020. Removal of phosphorus by aluminum-based drinking water treatment residuals collected from various geographic locations in the United States. *Geol. Soc. Am. Abstr. Program* 52 (6).
- Rattanaoudom, R., Visvanathan, C., Boontanon, S.K., 2012. Removal of concentrated PFOS and PFOA in synthetic industrial wastewater by powder activated carbon and hydrotalcite. *J. Water Sustain.* 2 (4), 245–258.
- Schmitt, G.L., Pietrzyk, D.J., 1985. Liquid chromatographic separation of inorganic anions on an alumina column. *Anal. Chem.* 57 (12), 2247–2253.
- Soleimanifar, H., Deng, Y., Wu, L., Sarkar, D., 2016. Water treatment residual (WTR)-coated wood mulch for alleviation of toxic metals and phosphorus from polluted urban stormwater runoff. *Chemosphere* 154, 289–292.
- Steigerwald, J.M., Ray, J.R., 2021. Adsorption behavior of perfluorooctanesulfonate (PFOS) onto activated spent coffee grounds biochar in synthetic wastewater effluent. *J. Hazard. Mater. Lett.* 2, 100025.
- Ünlü, N., Ersoz, M., 2006. Adsorption characteristics of heavy metal ions onto a low cost biopolymeric sorbent from aqueous solutions. *J. Hazard. Mater.* 136 (2), 272–280.
- USEPA, 2016. Drinking Water Health Advisories for PFOA and PFOS.
- Wang, F., Shih, K., 2011. Adsorption of perfluorooctanesulfonate (PFOS) and perfluorooctanoate (PFOA) on alumina: influence of solution pH and cations. *Water Res.* 45 (9), 2925–2930.
- Wang, F., Liu, C., Shih, K., 2012. Adsorption behavior of perfluorooctanesulfonate (PFOS) and perfluorooctanoate (PFOA) on boehmite. *Chemosphere* 89 (8), 1009–1014.
- Wang, Y., Niu, J., Li, Y., Zheng, T., Xu, Y., Liu, Y., 2015. Performance and mechanisms for removal of perfluorooctanoate (PFOA) from aqueous solution by activated carbon fiber. *RSC Adv.* 5 (106), 86927–86933.
- Wang, M., Orr, A.A., Jakubowski, J.M., Bird, K.E., Casey, C.M., Hearon, S.E., et al., 2021. Enhanced adsorption of per-and polyfluoroalkyl substances (PFAS) by edible, nutrient-amended montmorillonite clays. *Water Res.* 188, 116534.
- Willemsen, J.A., Bourg, I.C., 2021. Molecular dynamics simulation of the adsorption of per-and polyfluoroalkyl substances (PFASs) on smectite clay. *J. Colloid Interface Sci.* 585, 337–346.
- Xiao, X., Ulrich, B.A., Chen, B., Higgins, C.P., 2017. Sorption of poly-and perfluoroalkyl substances (PFASs) relevant to aqueous film-forming foam (AFFF)-impacted groundwater by biochars and activated carbon. *Environ. Sci. Technol.* 51 (11), 6342–6351.
- Xing, D.Y., Chen, Y., Zhu, J., Liu, T., 2020. Fabrication of hydrolytically stable magnetic core-shell aminosilane nanocomposite for the adsorption of PFOS and PFOA. *Chemosphere* 251, 126384.
- Xu, C., Chen, H., Jiang, F., 2015. Adsorption of perfluorooctane sulfonate (PFOS) and perfluorooctanoate (PFOA) on polyaniline nanotubes. *Colloids Surf. A Physicochem. Eng. Asp.* 479, 60–67.
- Xu, B., Liu, S., Zhou, J.L., Zheng, C., Jin, W., Chen, B., et al., 2021. PFAS and their substitutes in groundwater: occurrence, transformation and remediation. *J. Hazard. Mater.*, 125159.
- Yu, Q., Zhang, R., Deng, S., Huang, J., Yu, G., 2009. Sorption of perfluorooctane sulfonate and perfluorooctanoate on activated carbons and resin: kinetic and isotherm study. *Water Res.* 43 (4), 1150–1158.
- Zhang, D., He, Q., Wang, M., Zhang, W., Liang, Y., 2019a. Sorption of perfluoroalkylated substances (PFASs) onto granular activated carbon and biochar. *Environ. Technol.* 1–12.
- Zhang, D.Q., Zhang, W.L., Liang, Y.N., 2019b. Adsorption of perfluoroalkyl and polyfluoroalkyl substances (PFASs) from aqueous solution - a review. *Sci. Total Environ.* 694, 133606.
- Zhao, L., Bian, J., Zhang, Y., Zhu, L., Liu, Z., 2014. Comparison of the sorption behaviors and mechanisms of perfluorosulfonates and perfluorocarboxylic acids on three kinds of clay minerals. *Chemosphere* 114, 51–58.
- Zhou, Q., Deng, S., Zhang, Q., Fan, Q., Huang, J., Yu, G., 2010. Sorption of perfluorooctane sulfonate and perfluorooctanoate on activated sludge. *Chemosphere* 81 (4), 453–458.
- Zhou, L., Wallace, S.M., Denslow, N.D., Gaillard, J.F., Meyer, P., Bonzongo, J.C.J., 2021. A screening approach for the selection of drinking water treatment residuals (DWTRs) for their introduction to marine systems. *Environ. Toxicol. Chem.* 40, 1194–1203.
- Zhu, H., Jia, Y., Wu, X., Wang, H., 2009. Removal of arsenic from water by supported nano zero-valent iron on activated carbon. *J. Hazard. Mater.* 172 (2), 1591–1596.